Ferrocene in Conjugation with a Fischer Carbene: Synthesis, NLO, and Electrochemical Behavior of a Novel Organometallic Push−Pull System#

K. N. Jayaprakash,† Paresh C. Ray,§ Isao Matsuoka,¶ Mohan M. Bhadbhade,‡ Vedavathi G. Puranik,‡ Pushpendu K. Das,§ Hiroshi Nishihara,¶ and Amitabha Sarkar*,†

Division of Organic Chemistry (Synthesis) and Physical Chemistry Division, National Chemical Laboratory, Pune 411008, India, Department of Inorganic and Physical Chemistry, Indian Institute of Science, Bangalore 560012, India, and Department of Chemistry, School of Science, The University of Tokyo, Hongo, Bunkyo-ku, Tokyo 113-0033, Japan

Received April 12, 1999

Using an iterative sequence of Wittig olefination, reduction, oxidation, and condensation of an active methylene group to carbonyl, it was possible to prepare a series of organometallic push−pull molecules [$(CO)_5M{=}C(OCH_3)(-CH{=}CH-)_n(C_5H_4)Fe(C_5H_5)$, M = W, Cr, $n = 1-4$] in which ferrocene is the donor element and a Fisher carbene moeity is the acceptor group. The molecular first hyperpolarizability β was determined by hyper-Rayleigh scattering experiments. The β values ranged from 110×10^{-30} to 2420×10^{-30} esu in acetonitrile, and they are among the highest reported for organometallic molecules so far. Electrochemical measurements are consistent with the push−pull nature of these compounds.

Introduction

Synthesis of new organic and organometallic "push−pull" molecules has been intensively pursued in recent years in view of their useful material properties. The donor−acceptor substituted π-conjugated organic molecules possessing low-lying charge-transfer excited states are known to exhibit large second-order optical nonlinearities.[1] Most of the known NLO chromophores are based on substituted benzene, stilbene, or azobenzene derivatives, and extension of the π-conjugation connecting donor and acceptor moieties has resulted in exceptionally large β values.[2] Of late, optical nonlinearities of highly polarizable organometallic complexes have been investigated, though some investigators have dealt with only bulk material responses. Recent examples include organometallic and coordination complexes of almost all transition metals.[3,4]

Ferrocene complexes have been studied extensively in this context. Most of the ferrocene complexes that are investigated for their microscopic nonlinearity consist of ferrocene as a donor and an organic moiety such as $-NO_2$, $-CN$, $-CHO$, or $-CO_2Me$ substituted benzene, stilbene, or azobenzene derivatives as an acceptor.[4a,b,k,l] There are only a few recent reports[4i−l] where metallo-complexes act both as an acceptor and a donor.

In this paper, we report a novel series of organometallic polyene complexes containing ferrocene as a donor and a Fischer carbene complex of chromium or tungsten as an acceptor. The $M(CO)_5$ group, where M is Cr or W, behaves like a large electron-depleted group since the five CO ligands are strong π-acceptors. The choice of Fischer carbene complexes as a "pull" group in an organometallic push−pull complex for improved second-order NLO response is, therefore, a rational one.[5] The length of the polyene backbone has been varied in order to determine the chain length dependence of the first hyperpolarizability, β, of these complexes. An additional interest was to find out if the conjugated polyene linker

Dedicated to Professor D. Nasipuri on the occasion of his 75th birthday.

† Division of Organic Chemistry, NCL.

‡ Physical Chemistry Division, NCL.

§ Indian Institute of Science.

¶ The University of Tokyo.

(1) (a) Chemla, D. S. In *Nonlinear Optical Properties of Organic Materials and Crystals;* Zyss, J., Ed.; Academic Press: New York, 1987; Vols. 1 and 2. (b) *Introduction to Nonlinear Optical Effects in Molecules and Polymers*; Prasad, P. N., Williams, D. J., Eds.; John Wiley & Sons: New York, 1991. (c) Marder, S. R.; Sohn, J. E., *Material for Nonlinear Optics: Chemical Prespectives*; Stucky, G. D., Ed.; ACS Symposium Series 455; American Chemical Society: Wasington, DC, 1991.

(2) (a) Marder, S. R.; Perry, W. J.; Bourhill, G.; Gorman, B. C.; Tiemann, B. G.; Mansour, K. *Science* **1993**, 261, 186. (b) Rao Pushkara, V.; Jen, A. K. Y.; Wong, K. Y.; Drost, K. J. *J. Chem. Soc., Chem. Commun.* **1993**, 1118.

(3) (a)Long, N. J. *Angew. Chem., Int. Ed. Engl.* **1995**, 34, 21. (b) Whittall, I. R.; Mcdonagh, A. M.; Humphrey, M. G.; Samoc, M. In *Advances in Organometallic Chemistry*; Gordon, F., Stone, A., Eds.; Academic Press: San Diego, 1998; Vol. 42, p 291.

(4) (a) Green, M. L.; Marder, S. R.; Thomson, M. E.; Bandy, J. E.; Bloor, D.; Kolinsky, P. V.; Jones, R. J. *Nature* **1987**, *330*, 360. (b) Blanchard-Desce, M.; Runser, C.; Fort, A.; Barzoukas, M.; Lehn, J. M.; Bloy, V.; Alain, V. *Chem. Phys.* **1995**, *199*, 253. (c) Zyss, J.; Dhenaut, C.; Chauvan, T.; Ledoux, I. *Chem. Phys. Lett.* **1993**, *206*, 409. (d) Di Bella, S.; Fragala, I.; Ledoux, I.; Marks, T. J. *J. Am. Chem. Soc.* **1995**, *117*, 9481. (e) Ledoux, I.; Brasselet, S.; Dhenaut, C.; Zyss, J. In *Photoactive Organic Materials;* Kajzar, F., Agranovich, V. M., Lee, C. Y., Eds.; NATO ASI Series; Kluwer: The Netherlands, 1996; Vol. 9. (f) LeCours, S. M.; Guan, H. W.; DiMangno, S. G.; Wang, C. H.; Therien, M. J. *J. Am. Chem. Soc.* **1996**, *118*, 1495. (g) Houbrechts, S.; Clays, K.; Persoons, A.; Cadierno, V.; Gamasa, P. M.; Gimeno, J. *Organometallics* **1996**, *15*, 5266. (h) Sen, A.; Ray, P. C.; Das, P. K.; Krishnan, V. *J. Phys. Chem.* **1996**, *100*, 19611. (i) Calabrese, C. J.; Cheng. L. T.; Green, J. C.; Marder, S. R.; Tam, W. *J. Am. Chem. Soc.* **1991**, *113*, 7227. (j) Coe, B. J.; Houbrechts, S.; Asselberghs, I.; Persoons, A. *Angew. Chem., Int. Ed.* **1999,** *38*, 366. (k) Balavione, G. G. A.; Daran, J. C.; Iftime G.; Lacroix, P. G.; Manoury, E.; Delaire, J., A.; Maltey-Fanton, I.; Nakatani, K.; Bella, S. D. *Organometallics* **1999**, *18*, 21. (l) Lee, I. S.; Seo, H.; Chung, Y. K. *Organometallics* **1999**, *18*, 1091.

10.1021/om990257+ CCC: $18.00
Publication on Web 09/13/1999

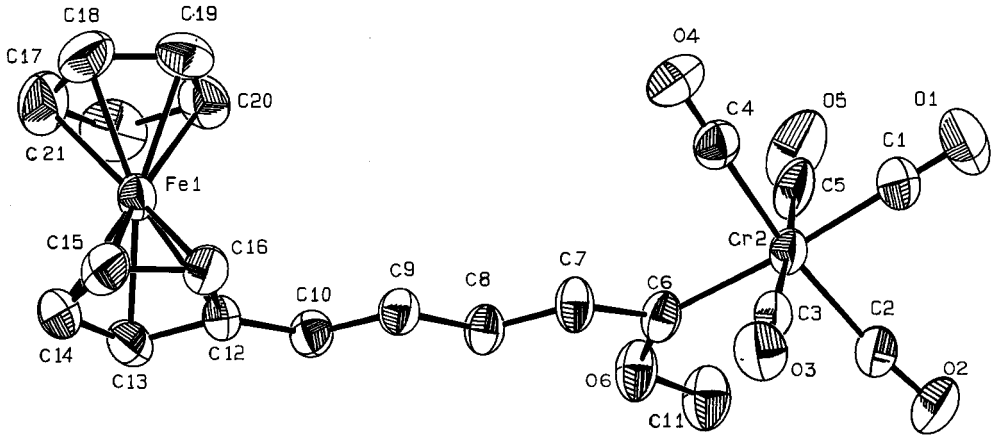

Figure 1. ORTEP diagram of complex **2b**.

Scheme 1

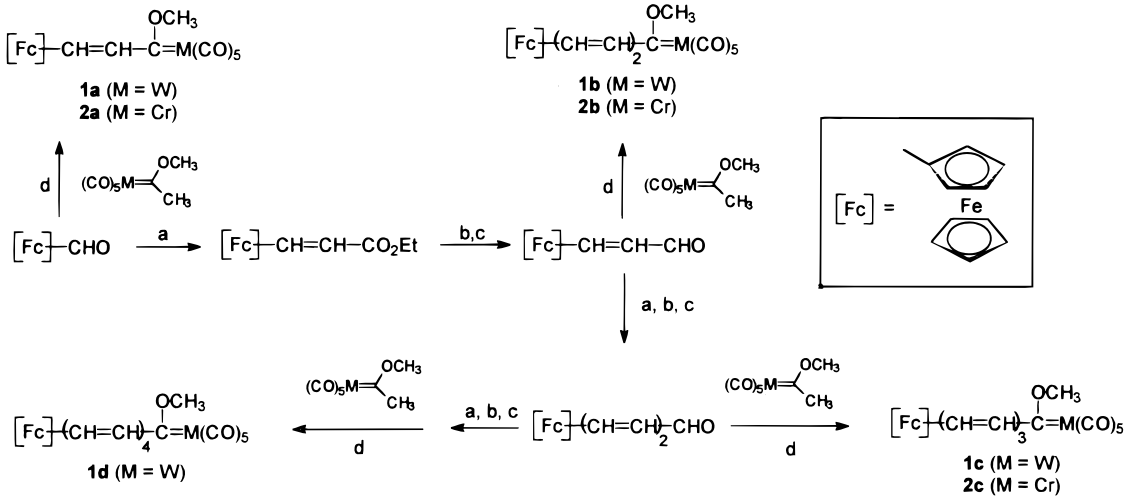

a: NaH / $(C_2H_5O)_2P(O)CH_2COOEt$, C_6H_6, 5 - 25 °C b: $LiAlH_4$ / $AlCl_3$, Ether, -15 to 25 °C

c: MnO_2 / CH_2Cl_2. rt d: Et_3N / TMSCl, Ether, rt

would act as a communication channel between the two metal centers with respect to electrochemical perturbations. The present study, therefore, focuses on the synthesis, structural characterization, linear optical spectroscopic properties, second-order NLO response, and electrochemical behavior of these complexes.

Results and Discussion

Synthesis of Metal Complexes. The general synthetic scheme for the preparation of organometallic "push−pull" polyenes is outlined in Scheme 1. Incremental addition of a =CH−CHO unit to ferrocene carboxaldehyde was effected in three steps: Wittig−Horner olefination to obtain the unsaturated ester, reduction of the ester to alcohol using aluminum hydride, and oxidation of this allylic alcohol with manganese dioxide. Individual steps provided the products in respectable yields (about 80−90%). Condensation of the ferrocene-derived aldehydes with methyl methoxy carbene complex was carried out following Aumann's procedure.[9] Yields of this step were limited to 40−50% only, and the more conjugated compounds were less stable. All new compounds were characterized by their ^1H and ^{13}C NMR spectral data and satisfactory elemental analysis.

Crystal Structure of Complex 2b. The crystal structure of a representative complex **2b** validated the structural assignment of these complexes (Figure 1, Tables 1 and 2). The presence of all-trans double bonds

(5) Calculations[6] show that a resultant positive charge is located on the metal of the Fischer carbene complex. In fact attack by nucleophiles at the carbene carbon is a major feature for these carbene complexes.[7a,b] The remarkable rate enhancement[8] of the Diels−Alder reaction of alkyne carbene complexes with dienes also testifies to the strong electron-withdrawing ("pull" effect) of the $M(CO)_5$ moeity. For previous use of Fischer carbene complexes as NLO materials, see: (a) Maiorana, S.; Papagni, A.; Licandro, E.; Persoons, A.; Clays, K.; Houbrechts, S.; Porzio, W. *Gazz. Chim. Ital.* **1995**, *125*, 377. (b) Fischer, H.; Podschadly, O.; Roth, G.; Herminghaus, S.; Klewitz, S.; Heck, J.; Houbrechts, S.; Meyer, T. *J. Organomet. Chem.* **1997**, *541*, 321. (c) Roth, G.; Fischer, H.; Meyer-Friendrichsen, T.; Heck, J.; Houbrechts, S.; Persoons, A. *Organometallics* **1998**, *17*, 1511.

(6) Nakatsuji, H.; Ushio, J.; Han, S.; Yonezawa, T. *J. Am. Chem. Soc.* **1983**, *105*, 426.

(7) (a) Hofman, P. In *Electronic Structures of Transition Metal Carbene Complexes*; Dotz, K. H., Fischer, H., Hofman, P., Kreissel, F. R., Schubert, U., Weiss, K., Eds.; Verlag-Chemie: Weinheim, 1983. (b) Connor, J. A.; Jones, E. M.; Lloyd, J. P. *J. Organomet. Chem.* **1970**, *24*, C20.

(8) Wulff, W. D.; Yang, D. C. *J. Am. Chem. Soc.* **1984**, *105*, 6726.

(9) Aumann, R.; Heinen, H. *Chem. Ber.* **1987**, *120*, 537.

Table 1. Crystallographic Data and Structure Refinement for $C_{21}H_{16}CrFeO_6$ (2b)

chemical formula	$C_{21}H_{16}CrFeO_6$
fw	472.19
crystal color	dark brown
crystal size (mm)	0.45 × 0.20 × 0.04
temperature (K)	295
radiation used λ (Å)	Mo Kα (0.7107) [graphite monochromatized]
crystal system	monoclinic
space group	$P2_1/a$
a (Å)	13.500(4)
b (Å)	11.856(4)
c (Å)	13.558(5)
β (deg)	108.13(3)
volume (Å^3)	2062.3(12)
ρ_{calcd} (Mg m^{-3})	1.521
Z	4
abs coeff, μ (mm^{-1})	1.264
θ range for data collection (deg)	2−22.5
no. of reflns collected	2972
no. of indep reflns	2700
F(000)	960
refinement method	full-matrix least-squares on F^2
type of diffractometer	Enraf Nonius CAD-4
scan mode	$\omega/2\theta$
scan speed	1 deg/min
final R indices [$I > 2\sigma(I)$]	R1 = 0.0323, wR2 = 0.0788
largest diff peak and hole	0.293 and −0.174 e Å^{-3}

Table 2. Selected Bond Lengths and Bond Angles of the Complex 2b

selected bond lengths in Å		selected bond angles in deg	
Cr1−C1	1.881(4)	C1−Cr1−C6	174.8(2)
Cr1−C2	1.913(4)	C6−O6−C7	38.3(2)
Cr1−C3	1.908(4)	C6−O6−C11	121.5(3)
Cr1−C4	1.886(4)	C7−O6−C11	159.8(3)
Cr1−C5	1.900(5)	Cr1−C6−O6	131.6(3)
Cr1−C6	2.051(4)	Cr1−C6−C7	121.1(3)
O6−C6	1.331(5)	C6−C7−C8	125.6(4)
C6−C7	1.462(5)	C7−C8−C9	125.1(4)
C7−C8	1.343(5)	C8−C9−C10	122.7(4)
C8−C9	1.439(5)	C9−C10−C12	127.6(4)
C9−C10	1.328(5)	C10−C12−C13	125.5(4)
C10−C12	1.447(5)	C10−C12−C16	127.8(3)
		C13−C12−C16	106.5(3)

in this molecule was confirmed. The structure displayed an extended conformation of the molecule, where the double bonds and the carbene−metal bond remained nearly coplanar [dihedral angles: C(9)−C(10)-C(12)−C(16) = 4.4(7); C(9)−C(10)-C(12)−C(13) = −179.6(4); C(8)−C(9)−C(10)−C(12) = −179.1(4); C(7)−C(8)−C(9)−C(10) = 176.9(4); C(6)−C(7)−C(8)−C(9) = −175.7(4); C(6)−O(6)−C(7)−C(8) = 171.4(4)]. The single bonds and the double bonds of the polyene link are characteristically different (1.439−1.462 vs 1.328−1.343 Å), indicating a limited π-delocalization in the ground state. Extensive delocalization over a π-framework has been observed earlier[5b] in amino carbene complexes where the $M(CO)_5$ and amino groups are separated by cumulated double bonds. The current structures differ on two counts: (a) these are methoxy carbene complexes where resonance participation of the oxygen lone pair is less, and (b) the methoxy group is attached to the carbene carbon itself, so it does not augment the "push" effect of ferrocene significantly.

UV−Visible Spectra. The electronic absorption spectra of ferrocene and substituted ferrocenes have been studied in the past.[4b,i] In ferrocene, the d_{z^2} orbital centered on the metal is generally accepted as the HOMO, and the combination of d_{xz} and d_{yz} is the LUMO. The absorption around 440 nm in ferrocene is assigned as the $^1E_{1g} \leftarrow {}^1A_{1g}$ transition. A higher energy band around 325 nm has been assigned as the $^1E_{2g} \leftarrow {}^1A_{1g}$ transition. The spectrum changes drastically upon substitution of the Cp ring with conjugated acceptor groups.

All the compounds studied here show two major absorption bands in the visible region (Figure 2).

The less intense band around 550 nm is due to the metal-to-ligand charge transfer (MLCT) mainly centered on ferrocene. This band does not shift appreciably with change in the number of double bonds in conjugation. Another sharper and more intense band (ca. 450 nm) arises from the $\pi-\pi^*$ transition in the polyene. This band shifts from 442 to 541 nm (shift of about 100 nm) when the number of double bonds between donor and acceptor increases from 1 to 4. It is noteworthy that the MLCT band shifts slightly to the blue in the tungsten complexes and to the red in the chromium complexes with increase in the conjugation length. The extinction coefficient measured at 532 nm also increases with conjugation, which is perhaps due to the overlap of these two bands (the bandwidth of the $\pi-\pi^*$ transition increases with conjugation). There is a third, weaker MLCT band in the ultraviolet (∼350 nm) originating from the metal carbonyl moiety. This band is far removed from resonance at the second-harmonic wavelength and will be ignored in our discussion here.

First Hyperpolarizability of Organometallic Complexes. Measurement of first hyperpolarizability of the new carbene complexes, **1** and **2**, was of immediate interest. We have examined how the nonlinearity−transparency tradeoff can be optimized by modifying the nature of the metal center as well as the length of the polyene linker in these bimetallic push−pull compounds.

Table 3 lists the first microscopic hyperpolarizabilities of all the compounds. Some of the compounds show much higher β values than DR1 (Disperse Red-1, $\beta = 165 \times 10^{-30}$ esu). The first hyperpolarizability changes drastically with the length of the polyene chain.

Since the molecules absorb around 532 nm the resonance contribution to β should be considered. An estimation of the dispersion-corrected component of β (that is, β_0), which is desired in such cases, cannot be made using the well-known two-state mode[10] since the UV−vis absorption spectra exhibit two distinct bands that are both close to the second-harmonic wavelength, and we cannot identify the excited state that contributes substantially to the resonant component of β. Also we have shown earlier[11a,b] that for a π-backbone with three or more double bonds between strong push−pull groups at the terminal positions a two-state description of nonlinearity is inadequate, although this model has been used in a similar context in the past to estimate average β_0 values for push−pull ferrocenyl polyenes.[4b]

(10) Oudar, J. L. *J. Chem. Phys.* **1977**, *67*, 446. For a crude estimation of static hyperpolarizability we have used the two-state model and obtained $|\beta_0|$ values for **1a**−**d** as 9.03, 29.77, 54.15, and 100.78, respectively. Similar values obtained for **2a**−**c** are 6.08, 21.05, and 45.35, respectively.

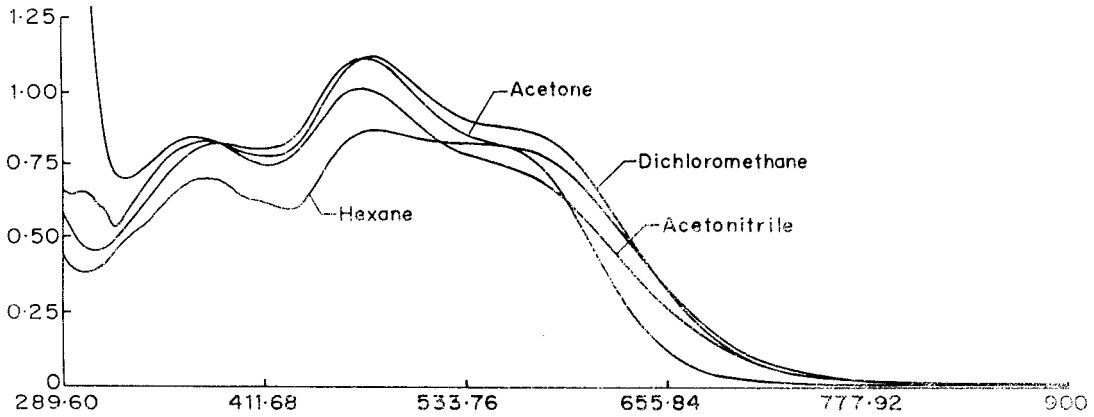

Figure 2. UV/vis spectra of **1c** in various solvents.

Table 3. Absorption Data and First Hyperpolarizability in Hexane for Complexes 1 and 2[a]

compound	n	λ_{max} (nm)	$\epsilon_{532} \times 10^4$ (L mol^{-1} cm^{-1})	$\langle\beta\rangle$ ($\times 10^{-30}$ esu (±8%))
1a	1	558.8	9512	66.8
		442.6		
1b	2	558.2	16577	220.4
		463.4		
1c	3	550.9	23723	408.0
		486.4		
1d	4	541.4	29100	780.4
2a	1	543.2	11933	46.8
		462.8		
2b	2	546.3	16630	160.6
2c	3	549.6	23940	342.8

[a] Molar concentrations used for the measurements were in the range 10^{-5}–10^{-7}; *p*-nitroaniline, for which β (chloroform) = 24.5 $\times 10^{-30}$ esu, was used as external reference.[18]

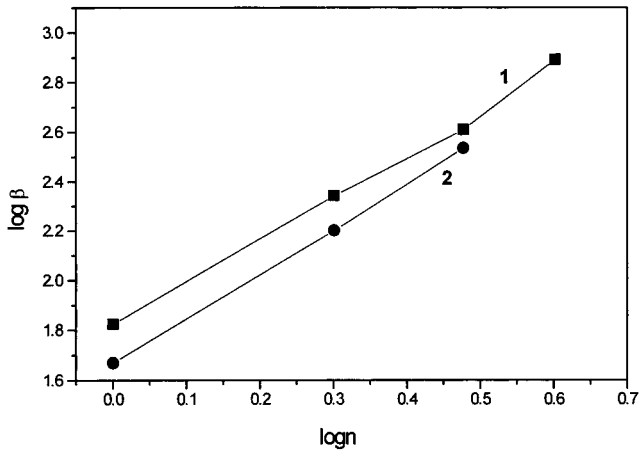

Figure 3. Plot of log β values against logarithm of the number of double bonds, *n*, of the polyene chain for the tungsten (squares) and chromium (circles) complexes.

For W and Cr complexes of equal conjugation length, the former exhibits higher nonlinearity. In fact, the W complexes are expected to have higher hyperpolarizability as a result of more efficient back-donation to the CO ligand from the metal. The efficiency of back-donation is reflected in the relative bond strength of Cr–CO and W–CO bonds (108 and 178 kJ/mol).[12] Since the λ_{max} of the ferrocene-centered MLCT band does not correlate with the trend in β, it perhaps contributes less to the first hyperpolarizability of these complexes. On the other hand β increases with the λ_{max} corresponding to the π–π^* transition. This implies that the charge-transfer excited states that contribute substantially (resonant or near resonant) to β also increase with increasing conjugation length, as to be expected. Calculations[11a,b] predict a nonlinear dependence of β on the conjugation length. In other words, in extended conjugated systems the number of excited states contributing to β increases with length of the π-backbone.[11c] Using a relationship $\beta = an^b$ (where *a* and *b* are constants and *n* is the number of double bonds), we find from the plot of log β vs log *n* (Figure 3) that the exponent *b* is 1.74 for the tungsten compounds and 1.81 for the chromium complexes. The value of the exponent for the series is higher than that of the simple ferrocenyl polyenes terminated with an aldehyde group (1.60).[4b] Since the slope for tungsten complexes is lower than corresponding chromium complexes, after a certain chain length a reversal of observed trends may be expected.

The first hyperpolarizability of these bimetallic push–pull polyenes exhibits significant solvent polarity dependence. Table 4 lists β values for all compounds in four different solvents.

It is interesting to note that the value of β increases approximately by a factor of 3 when the solvent dielectric constant changes by a factor of 20. The first hyperpolarizability of **1d** in acetonitrile is 2420 $\times 10^{-30}$ esu, one of the largest values reported for an organometallic compound. The largest β reported so far belongs to a zinc–porphyrin complex.[4f] The enhancement of β in these molecules is not due to any significant increase in the resonance contribution (see, for example, ref 4j), as seen from solvatochromic shifts of the absorption spectra. In fact, the wavelength of π–π^* absorption maximum shifts merely 20–30 cm^{-1} from hexane to acetonitrile. Also the absorption coefficient at 532 nm (ϵ_{532}) decreases as we go from a solvent dielectric constant of 1.9 (hexane) to 37.5 (acetonitrile). This suggests that, in a polar solvent, charge transfer from

(11) (a) Ramasesha, S.; Das, P. K. *Chem. Phys.* **1990**, *145*, 343. (b) Albert, I. D. L.; Das, P. K.; Ramasesha, S. *Chem. Phys. Lett.* **1990**, *168*, 454. (c) In all the compounds resonance enhancement contributes a part to β. The factors governing the resonance enhancement are not understood thoroughly. It is known that the stronger acceptor does not necessarily lead to the largest nonlinearities (see: Marder, S. R.; Gorman, G. B.; Tiemann B. G.; Cheng, L. T. *J. Am. Chem. Soc.* **1993**, *115*, 3006); rather an optimal degree of bond length alteration in a polyene bridge exhibits the largest β (see: Gorman, G. B.; Marder, S. R. *Proc. Natl. Acad. Sci. U.S.A.* **1993**, *90*, 11297).

(12) Foley, H. C.; Strubinger, L. M.; Targos, T. S.; Geoffroy, G. L. *J. Am. Chem. Soc.* **1983**, *105*, 3064.

Table 4. First Hyperpolarizability (β, $\times 10^{-30}$ esu) of Compounds 1 and 2 in Different Solvents (Dielectric Constant of the Solvent Is Shown in Parentheses)

compound	hexane ($D = 1.90$)		dichloromethane ($D = 9.10$)		acetone ($D = 20.7$)		acetonitrile ($D = 37.5$)	
	β	ϵ_{532}	β	ϵ_{532}	β	ϵ_{532}	β	ϵ_{532}
1a	67	9512	82	7959	102	6729	160	6257
1b	220	16577	402	10239	520	8677	600	7475
1c	408	23723	580	23444	840	20039	1140	18638
1d	780	29110	960	24422	1720	23642	2420	22950
2a	47	11933	69	8529	89	7002	110	6844
2b	161	16630	240	15477	306	12892	410	10532
2c	342	23940	440	17404	760	14617	1030	14322

ferrocene donor to Fischer carbene acceptor through the polyene backbone is facilitated unevenly both in the ground and the excited states. No fluorescence was observed for any of these compounds at 532 or 355 nm excitation.

Bulk Susceptibility. Since most of the molecules crystallize in centrosymmetric space groups, we were unable to measure the powder SHG using Kurtz powder technique. The macroscopic hyperpolarizabilities $\chi^{(2)}$ have been measured using the poled (corona onset) polymer technique.[13]

The macroscopic nonlinearity, d_{33} (that is, $\chi^{(2)}_{33/2}$), values of the NLO doped PMMA films were obtained using the following equation, disregarding the difference in the refractive indices of film and quartz:

$$d_{33}^{s}/d_{33}^{q} = n_s^{3/2}(I_{2\omega}^{s}/I_{2\omega}^{q})I_c^{q}/IFn_q^{3/2}$$

where I_c^q is the coherence length of quartz, I is the thickness of the doped polymer film, n_s is the refractive index of the sample, n_q is the refractive index of quartz, $I_{2\omega}^s$ and $I_{2\omega}^q$ are the second-harmonic intensities of the polymer film and quartz, respectively, and F is a factor which is 1.2 for our experimental conditions. Compounds **1d** and **2c** exhibit very large d_{33} values, 28 and 20 pm/V, respectively (measured with respect to Y-cut quartz having $d_{33} = 0.55$ pm/V). Even these values are the highest reported d_{33}'s for any organometallic compound. These high values also help us to conclude that the contribution of two-photon fluorescence is negligible in HRS intensity for our compounds.

Electrochemical Studies. Redox properties of the complexes are examined in order to evaluate the "push−pull" behavior of the ferrocene and Fischer carbene complex moieties. Cyclic voltammograms of **1b** and **2b** in Bu_4NClO_4−MeCN are displayed in Figure 4, showing two-step 1e$^-$ oxidation and irreversible 1e$^-$ reduction waves in the potential range between −1.75 and 0.6 V vs Fc/Fc^+ for both complexes. In the voltammogram of the W complex **1b**, a further irreversible oxidation wave is observed at $E_{p,a} = 0.787$ V (Figure 4a). The first-step oxidation at $E^{0'} = (E_{p,a} + E_{p,c})/2 = 0.083$ V for **1b** and 0.097 V for **2b** is reversible, suggesting that this oxidation should be ascribed to the ferrocene−ferrocenium couple. Also, the absorption spectrum of the solution of **2b** after electrolysis at 0.32 V shows a decrease in intensity of the band at 570 nm characteristic of MLCT mainly due to the ferrocene moiety as mentioned above and an appearance of a new band at 830 nm. This observation further supports oxidation of ferrocene in the first step. The second-step oxidation at $E_{pa} = 0.412$ V for **1b** and 0.490 V for **2b** and the irreversible reduction at $E_{pc} = -1.378$ V for **1b** and −1.394 V for **2b** can be ascribed to the Fischer carbene complex moiety since the authentic carbene complexes, $(CO)_5W{=}CMe(OMe)$ and $(CO)_5Cr{=}CMe(OMe)$ undergo similar oxidation reaction at $E_{pa} = 0.674$ and 0.453 V and irreversible reduction at $E_{pc} = -2.136$ and −2.130 V, respectively.[14] Similar two-step oxidation and single-step reduction waves in the cyclic voltammogram were

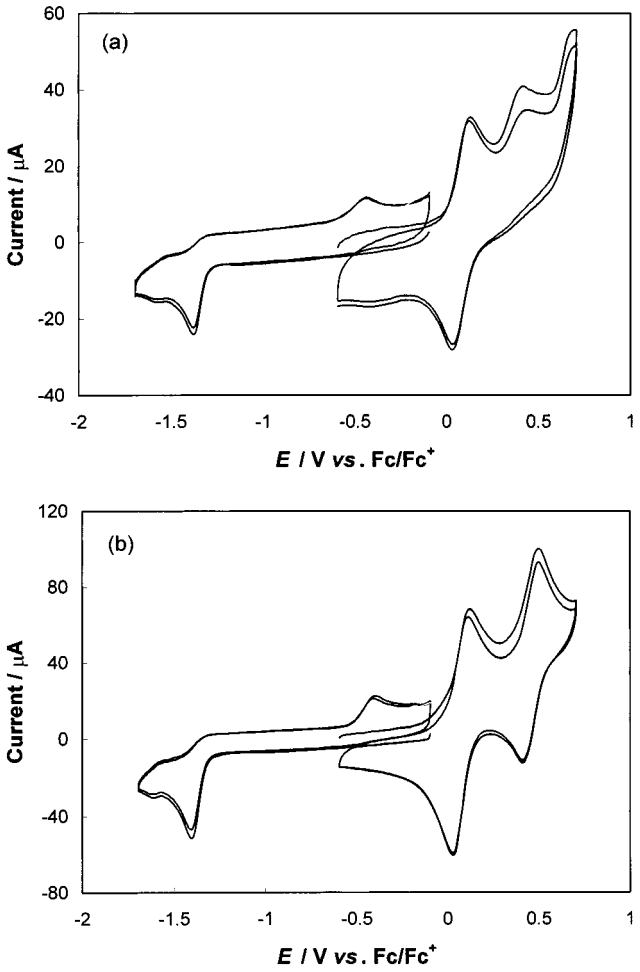

Figure 4. Cyclic voltammograms of **1b** (a) and **2b** (b) at glassy carbon in 0.1 M Bu_4NClO_4−MeCN at a scan rate of 0.1 V s^{-1} at 25 °C.

(13) (a) Marks, T. J.; Ratner, M. A. *Angew. Chem., Int. Ed. Engl.* **1995**, *34*, 155. (b) Ray, P. C.; Das, P. K. *Chem. Phys. Lett.* **1994**, *229*, 415.

(14) Similar data for electrochemical oxidation and reduction of carbene complexes have been reported separately by Lloyd et al.[15] and Casey et al.[16] Compared to the W complex, **1b**, the Cr complex **2b** shows higher reversibility of the second-step oxidation reaction. This difference in chemical reversibility is also observed for the authentic carbene complexes.

Table 5. Redox Properties of the Bimetallic Complexes[a]

	oxidation			reduction	
compound	1st $E^{0'}$	2nd E_{pa}	E_{pc}	$E^{0'}$	E_{pc}
1a	0.134	0.473			−1.583
1b	0.083	0.412			−1.378
2a	0.135	0.501	0.418	0.460	−1.617
2b	0.076	0.490	0.417	0.454	−1.394
2c	0.034	0.503	0.414	0.460	−1.286

[a] Measured in 0.1 M Bu_4NClO_4−MeCN. Potentials are given with respect to ferrocene/ferrocenium.

observed for other polyene-bridged bimetallic complexes, although their redox potentials depend on the length of the polyene and the metal of the Fisher carbene complex moiety. The electrochemical properties of **1a**, **1b**, **1c**, **2a,** and **2b** are summarized in Table 5.

Other things remaining equal, a change of metal in the carbene complex moiety has little effect on the first oxidation potential if one compares **1a** with **2a** and **1b** with **2b**. The oxidation potential and the reduction potential of the second step ascribed to the metal−carbene moiety depend on the metal present. The reduction potentials are less negative for the W complexes compared to the Cr complexes; that is, the electron-accepting ability of the W complexes is higher than the corresponding Cr complexes. This is in accordance with the higher hyperpolarizability of the W complexes as mentioned above. The effect of bridging polyene length on the redox potentials is significant for both the oxidation of the ferrocene moiety and the reduction of the carbene complex moiety, as represented in Table 3. For both of the W and Cr complexes, the first oxidation potential and the reduction potential shift in the less positive and less negative direction, respectively, with increasing the polyene length. This can be attributed to the change in electron-withdrawing effects of the carbene complex moiety on the ferrocene moiety *vis-à-vis* the electron-donating effect of the ferrocene moiety on the carbene complex moiety. Both the effects would decrease with increasing the distance between the carbene complex moiety and the ferrocene moiety, leading to the shift in redox potentials as noted above. These strong dependencies of the redox potentials on the polyene length suggest that the Fischer carbene and ferrocene moieties are electronically communicated significantly via the polyene linker and they behave as a strong donor−acceptor couple.

Conclusion

In summary, we have described a new series of bimetallic push−pull polyenes displaying significantly high second-order nonlinearity. It is clear from this study that the Fischer carbene moiety is a strong electron-withdrawing group in the context of NLO. The hyperpolarizability of the polyene systems increases as a function of the number of double bonds, as expected. In comparison with other NLO systems, the polyenic systems are still unequalled insofar as their second-order nonlinearity is concerned. One of the compounds reported here (**1d**) exhibits one of the highest microscopic nonlinearities measured for any organometallic complex. Very high β values of these bimetallic complexes make them promising NLO candidates for device applications. Electrochemical studies of the bimetallic complexes have revealed significant dependency of the redox potentials on the metal in the Fischer carbene complex moiety and on the polyene length. This is in accordance with the "push−pull" properties of the complexes.

Experimental Section

All reactions were performed under an inert atmosphere of argon. Solvents were dried using standard procedures and distilled under an inert atmosphere prior to use. Infrared spectra were obtained on a Perkin-Elmer 599B spectrometer in chloroform solution. The ^{1}H NMR spectra were recorded on Bruker AC-200 spectrometer, whereas ^{13}C NMR spectra were recorded on a Bruker AC-200 and Bruker AMX 500 spectrometers at 50.3 and 125.7 MHz, respectively, using $CDCl_3$ as the solvent and reported as parts per million downfield of tetramethylsilane. Absorption measurements were carried out on a Perkin-Elmer Lambda 15 UV/vis spectrophotometer with concentrations of $\sim 10^{-5}$ mol/L. Elemental analyses of compounds were carried out on a Carlo-Erba 1100 automatic analyzer. Melting points in the Celsius scale were determined in open capillary tubes on a Thermonik Campbell melting point apparatus and are uncorrected. Bu_4NClO_4 was supplied from Tomiyama Chemicals as lithium battery grade. UV−vis−NIR spectra of electrolysis products were recorded with a JASCO V-570 spectrometer.

Synthesis of Complexes. Wittig−Horner Reaction. To a benzene solution of the anion of diethyl acetyl phosphonate (*n* mmol) generated using equimolar amount of NaH was added aldehyde (*n* mmol) in benzene at 5−10 °C (ice−water mixture) After 1.5−2.0 h, the reaction was quenched with water. The product was extracted into ether and purified by chromatography (silica gel, 20% EtOAc in petroleum ether).

Aluminum Hydride Reduction. The aluminum hydride reagent generated from $LiAlH_4$ and $AlCl_3$ (molar ratio 3:1) in ether was added to an ether solution of unsaturated ester (equimolar) at −15 °C. After stirring for 1 h, the reaction mixture was quenched with water. Alkaline workup followed by chromatography afforded the allylic alcohol.

Manganese Dioxide Oxidation. Oxidation of the alcohol with 10 molar equiv of MnO_2 in dichloromethane furnished the unsaturated aldehyde, which was used without further purification.

Condensation of Aldehyde with Carbene Complexes. Following Aumann's procedure,[9] equimolar quantities of aldehyde and methyl methoxy carbene complex in ether with triethylamine (4 equiv) and trimethylsilyl chloride (3 equiv) were used, and the mixture was stirred for 24 h. Solvent was removed under reduced pressure, and the product was purified by flash chromatography.

Yields given here are overall yields after all four steps.

Compound **1a**: Yield 50%; mp 119 °C; IR 2035 (m), 1970 (sh), 1925 (s), 1575 (m) cm^{-1}; ^{1}H NMR ($CDCl_3$) δ 4.23 (s,5H), 4.57 (s,3H), 4.65 (s, 4H), 7.42 (s, 2H); ^{13}C NMR ($CDCl_3$) δ 68.49, 70.17, 70.65, 73.12, 78.66, 141.21, 143.46, 198.21, 204.02, 300.96. Anal. Calcd for $C_{19}H_{14}O_6FeW$: C, 39.48; H, 2.44. Found: C, 39.77; H, 2.64.

Compound **1b**: Yield 48%; mp 128 °C; IR 2060 (m), 1980 (sh), 1910 (s), 1565 (m) cm^{-1}; ^{1}H NMR ($CDCl_3$) δ 4.15 (s, 5H), 4.45−4.55 (m, 4H), 4.60 (s, 3H), 6.45 (dd, J = 15, 11.2 Hz, 1H), 6.95−7.10 (m, 2H), 7.30 (d, J = 15 Hz, 1H); ^{13}C NMR ($CDCl_3$) δ 68.61, 70.42, 71.60, 73.16, 81.22, 124.50, 137.22, 144.00, 147.51, 197.95, 204.09, 302.6. Anal. Calcd for $C_{21}H_{16}O_6FeW$: C, 41.76; H, 2.67; Found: C, 41.54; H, 3.00.

Compound **1c**: Yield 45%; mp 142 °C; IR 2060 (m), 1975 (sh), 1925 (s), 1540 (m) cm^{-1}; ^{1}H NMR ($CDCl_3$) δ 4.15 (s, 5H),

4.40−4.45 (m, 4H), 4.55 (s, 3H), 6.30 (dd, J = 15, 11.2 Hz, 1H), 6.5 (dd, J = 15, 11.2 Hz, 1H), 6.85 (m, 2H), 7.00 (dd, J = 15, 11.2 Hz, 1H), 7.30 (d, J = 14.5 Hz, 1H); ^{13}C NMR ($CDCl_3$) δ 68.10, 69.81, 70.28, 71.90, 81.75, 126.77, 128.65, 136.78, 139.06, 146.04, 147.20, 197.88, 204.07, 302.65. Anal. Calcd for $C_{23}H_{18}O_6FeW$: C, 43.84; H, 2.88. Found: C, 43.64; H, 3.05.

Compound **1d**: Yield 40%; mp 155 °C; IR 2060 (m), 1980 (sh), 1925 (s), 1530 (m) cm^{-1}; ^{1}H NMR ($CDCl_3$) δ 4.10 (s, 5H), 4.35−4.50 (m, 4H), 4.55 (s, 3H), 6.20−7.00 (m, 6H), 7.10 (dd, J = 15, 11.2 Hz, 1H), 7.30 (d, J = 15 Hz, 1H); ^{13}C NMR ($CDCl_3$) δ 67. 13, 69.51, 69.54, 70.38, 82.32, 126.77, 130.10, 135.0, 137.13, 139.10, 144.95, 145.10, 146.20, 197.84, 204.08, 302.75. Anal. Calcd for $C_{25}H_{20}O_6FeW$: C, 45.76; H, 3.07. Found: C, 46.00; H, 3.20.

Compound **2a**: Yield 53%; mp 122 °C; IR 2030(m), 1970 (sh), 1945 (s), 1575 (m) cm^{-1}; ^{1}H NMR ($CDCl_3$) δ 4.15 (s, 5H); 4.25 (s, 3H); 4.60−4.80 (m, 4H); 7.15 (d, J = 15 Hz, 1H); 7.50 (d, J = 15 Hz, 1H); ^{13}C NMR ($CDCl_3$) δ 65.10, 69.52, 69.90, 72.27, 77.90, 136.99, 138.15, 216.89, 223.93, 323.59. Anal. Calcd for $C_{19}H_{14}O_6CrFe$: C, 45.59; H, 2.13. Found: C, 45.30; H, 2.23.

Compound **2b**: Yield 45%; mp 138 °C; IR 2050 (m), 1975 (sh), 1935 (s), 1555 (m) cm^{-1}; ^{1}H NMR ($CDCl_3$) δ 4.20 (s, 5H), 4.45−4.60 (m, 4H), 4.70 (s, 3H), 6.40 (dd, J = 15,11.3 Hz, 1H), 6.80 (dd, J = 15, 11.3 Hz, 1H), 7.00 (d, J = 15 Hz, 1H), 7.35 (d, J = 15 Hz, 1H); ^{13}C NMR ($CDCl_3$) δ 67.88, 68.82, 69.79, 70.88, 81.13, 124.23, 132.90, 140.96, 147.77, 217.14, 224.58, 328.37. Anal. Calcd for $C_{21}H_{16}O_6CrFe$: C, 53.42; H, 3.42. Found: C, 53.75; H, 3.70.

Compound **2c**: Yield 43%; mp 163 °C; IR 2050 (m), 1980 (sh), 1925 (s), 1540 (m) cm^{-1}; ^{1}H NMR ($CDCl_3$) δ 4.15 (s, 5H), 4.40−4.50 (m, 4H), 4.70 (s, 3H), 6.30 (dd, J = 15, 11.30 Hz, 1H), 6.45−6.85 (m, 4H), 7.45 (d, J = 15 Hz, 1H); ^{13}C NMR ($CDCl_3$) δ 67.42, 68.02, 69.02, 70.74, 81.68, 125.96, 128.42, 132.79, 139.28, 141.68, 147.29, 217.10, 224.6, 328.30. Anal. Calcd for $C_{23}H_{18}O_6CrFe$: C, 55.45; H, 3.64. Found: C, 55.65; H, 3.90.

SHG Measurement. Microscopic second-order nonlinearities, β, of all the compounds in different solvents have been measured by hyper-Rayleigh scattering (HRS) technique.[17a−e] The experimental setup for the HRS technique has been described in detail elsewhere.[18a,b] In brief, the fundamental of a Q-switched Nd:YAG (Spectra Physics, 8 ns) is focused after 5 cm of a glass cell containing the solute in solution. The two-photon scattering signal is imaged efficiently in the perpendicular direction onto a visible sensitive photomultiplier tube (PMT). A 3 nm bandwidth, 532 nm interference filter is used on the signal path to isolate the second-harmonic light. A small fraction of the 1064 nm fundamental is directed toward an IR sensitive detector for monitoring the incident light intensity. Signals from both the PMTs are fed into a gated boxcar averager (SRS 250) to record the intensities of the incident and second-order scattered light pulses after averaging over 1000 shots. All data are collected at laser powers (≤2 mJ/pulse) well below the threshold for stimulated Raman, self-focusing, Brillouin scattering, and dielectric breakdown.

The theory of the harmonic light scattering has been developed by several authors.[19] For a mixture of two different species, e.g., for a solute and a solvent, the resulting second-harmonic intensity $I_{2\omega}$ is related to the incident laser intensity, I_ω, in the following way:

$$I_{2\omega} = G[N_{\text{solvent}}\beta_{\text{solvent}}{}^2 + N_{\text{solute}}\beta_{\text{solute}}{}^2]I_\omega 2 \ldots \qquad (1)$$

where G is an instrument factor, N_i is the number density of the ith species in solution, and β_i is the first hyperpolarizability. The quadratic coefficient $I_{2\omega}/I_\omega{}^2$ is a linear function of the number density, N_{solute}, of the solute, if β and N for the solvent are constant. The intercept can be used to calculate the proportionality factor G, provided β_{solvent} is known. The G factor depends on the wavelength, the distance between the cell and the detector, the solid angle of photon collection and the PMT gain. This approach effectively eliminates the need for the knowledge of local field factors since these factors are divided out by measuring at nearly the same local field. We have used PNA in chloroform (β = 24.5 × 10^{-30} esu) as an external reference for this experiment. Terhune et al.[17a] calibrated carbon tetrachloride with respect to quartz, using the same HRS technique, and we have calibrated all the solvents (used in this paper) by a method similar to that described by Zyss et al.[17d]

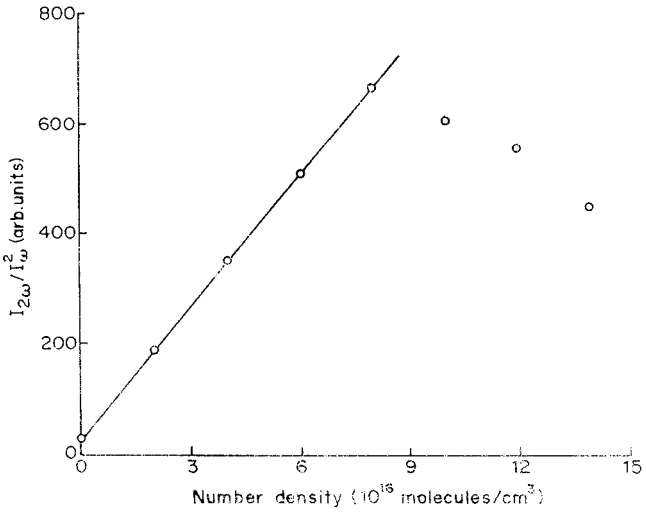

Figure 5. Quadratic coefficient $I_{2\omega}/I_\omega{}^2$ vs number density of compound **1a** in hexane.

In the case of absorption of the light scattered at 2ω by the NLO molecules, a correction term may be necessary.[18a]

$$I_{2\omega} = G[N_{\text{solvent}}\beta_{\text{solvent}}{}^2 + N_{\text{solute}}\beta_{\text{solute}}{}^2]I_\omega{}^2 \times 10^{\{-\epsilon(2\omega)Nl\}}$$

where $\epsilon(2\omega)$ is the absorption coefficient at the second-harmonic frequency, N is the number density of the absorbing molecules, and l is the effective optical path length. Figure 5 shows the $I_{2\omega}/I_\omega{}^2$ vs solute number density plot for compound **1a**.

The deviation from linearity at high concentrations of the solute is due to the self-absorption of the molecule at 532 nm. The slope and intercept of the plot at lower concentrations (the linear part of Figure 5) permit evaluation of β values, and we adopted this approach to obtain the values for compound **1a** as 66.8 × 10^{-30} esu in hexane. Similarly we obtained β values for the other compounds.

Bulk Susceptibility Measurements. The poly(methyl methacrylate)(PMMA) [$n(d)$ =1.4900 at 20 C, d = 1.188, MW = 280000) used in this study were purchased from Aldrich Chemical Co. and used with out further purification. We have doped 5 wt % of NLO organometallic chromophore in PMMA. The experimental apparatus for corona poling has been described elsewhere.[13b] Briefly, plane-polarized 1064 nm light from an Nd:YAG laser (spectra Physics, DCR-11, 10 Hz, 100−150 mJ/10 ns pulse) was incident on the sample. After rejecting

(15) Lloyd, M. K.; McCleverty, J. A.; Orchard, D. G.; Connor, J. A.; Hall, M. B.; Hillier, I. H.; Jones, E. M.; McEwen, G. K. *J. Chem. Soc., Dalton Trans.* **1973**, 1743.

(16) Casey, C. P.; Albin, L. D.; Saeman, M. C.; Evans, D. H. *J. Organomet. Chem.* **1978**, *155*, C37.

(17) (a) Terhune, R. W.; Maker, P. D.; Savage, C. M. *Phys. Rev. Lett.* **1965**, *14*, 681. (b) Clays, K.; Persoons, A. *Phys. Rev. Lett.* **1991**, *66*, 2980. (c) Clays, K.; Persoons, A. *Rev. Sci. Instrum.* **1992**, *63*, 3285. (d) Zyss, J.; Van, T. C.; Dhenaut, C.; Ledoux, I. *Chem. Phys.* **1993**, *177*, 281. (e) Lambert, C.; Strefan, S.; Bourhill, G.; Brauchle, C. *Angew. Chem., Int. Ed. Engl.* **1996**, *35*, 644.

(18) (a) Ray, P. C.; Das, P. K. *J. Phys. Chem.* **1995**, *99*, 14414. (b) Ray, P. C.; Das, P. K. *J. Phys. Chem.* **1995**, *99*, 17891.

(19) Clays, K.; Persoons, A.; De Mayer, L. *Adv. Chem. Phys.* **1994**, *85*, 445.

the fundamental wavelength (using $CuSO_4$ solution filter) the signal at 532 nm was collected on a UV−visible PMT. The output from the PMT was fed to a digital storage oscilloscope. The second-harmonic intensity was measured relative to a quartz plate ($I_c = 20.6$ mm and $d_{11} = 0.5$ pm/V). The dc electric field (6 kV) was applied through a needle electrode placed 1 cm above the ground planner aluminum electrode.

Electrochemical Measurements. A glassy carbon rod (outside diameter 5 mm, Tokai Carbon GC-20) was embedded in Pyrex glass, and a cross section was used as a working electrode. Cyclic voltammetry was carried out in a standard one-compartment cell under an argon atmosphere equipped with a platinum wire counter electrode and an Ag/Ag^+ reference electrode (10 mM $AgClO_4$ in 0.1 M Bu_4NClO_4−MeCN, $E^{0'}$(ferrocene/ferrocenium in 0.1 M Bu_4NClO_4/CH_2Cl_2) = 0.214 V vs Ag/Ag^+) with a BAS CV-50W voltammetric analyzer.

X-ray Structure Solution of Complex 2b. The crystals of the complex **2b** were grown from petroleum ether−dichloromethane. The structure was solved using SHELX-86. Least-squrares refinement of scale factors and positional and anisotropic thermal parameters including hydrogen atoms were carried out using SHELXL-93.[20] The weighting scheme was $w = 1/[\sigma^2(F_o)^2 + (0.0478P)^2 + 0.00P]$, where $P = (F_o^2 + 2F_c^2)/3$. The refinement converged to $R = 0.0323$ for 2700 observed reflections.

(20) Sheldrick, G., M. *SHELXL93*: Program for crystal structure refinement; University of Gottingen: Gottingen, Germany, 1993.

Acknowledgment. This work was supported by Department of Science & Technology, Govt. of India, and partly funded by the All India Council for Technical Education, Govt. of India. J.K.N. and P.C.R. thank the CSIR, New Delhi, for Research Fellowships. The authors thank the National Facility for High-field NMR at TIFR, Mumbai, for providing the high-field spectra reported in this paper.

Supporting Information Available: Details about the X-ray crystal structures, including ORTEP diagrams and tables of crystal data and structure refinement, atomic coordinates, bond lengths and angles, and anisotropic displacement parameters for **2b**. This material is available free of charge via the Internet at http://pubs.acs.org.

OM990257+